

# X-ray study of heterogeneous nucleation of dislocations in P-diffused silicon

C. GHEZZI

Laboratorio MASPEC del C.N.R., Parma, Italy

M. SERVIDORI

Laboratorio LAMEL del C.N.R., Bologna, Italy

X-ray topography was employed in order to study the nucleation of dislocation lines at surface heterogeneities in (111) Si wafers during phosphorus diffusion. Star-like patterns of 60° dislocations nucleated at phosphorus decorated surface defects were observed and were proved to be localized within the diffused layer. The analysis of the X-ray contrast and the results of some heating experiments suggested a mechanism of growth of the dislocation lines which was based on climb processes.

## 1. Introduction

Phosphorus diffusion is a widely used process in planar technology of silicon devices and a great deal of effort has been made in order to clarify the generation mechanisms of various crystallographic defects produced during the process itself. One of the most commonly used techniques is X-ray topography, owing to its non-destructive peculiarity. As regards the generation of dislocation lines, the attention was mainly devoted to homogeneous nucleation processes. In this case, lattice parameter variations accompanying gradients in the solute concentration cause internal stresses in the crystal; if these exceed the yield stress, plastic relaxation introduces an array of dislocations [1, 2]. This mechanism has been related to a sufficiently high concentration of the dopant impurities.

On the other hand, when discussing the generation of dislocations, one has to take into account the presence of concentrations of elastic stresses localized at precipitates, scratches, cracks and, more generally, at surface heterogeneities. In these cases, the correlation between the dopant concentration and the presence of dislocation lines is no more significant. The problem of heterogeneous nucleation of dislocations and stacking faults has been studied by means of transmission electron microscopy and chemical etching [3-6], whereas there is no evidence in the literature of similar investigations performed by X-ray methods.

The present paper is concerned with an X-ray

study on heterogeneous nucleation of dislocations in (111) phosphorus diffused Si wafers. The application of Lang topography was made possible by the presence of few sources of dislocation lines.

## 2. Experimental methods

The samples we used in all the experiments were Czochralski pulled (111) Si wafers of p-type ( $\rho \sim 1 \Omega\text{-cm}$ ). The predeposition process was performed at  $T = 1000^\circ\text{C}$  for 25 and 50 min in a 94%  $\text{N}_2$  and 6%  $\text{O}_2$  atmosphere, with  $\text{POCl}_3$  as the source for P impurities. The sheet resistivity of the diffused layer was measured after the predeposition step as well as after a drive-in process made at  $1100^\circ\text{C}$  for 1 h. Two values,  $Q_1$  and  $Q_2$ , of the total amount of phosphorus which was electrically active were found; since  $Q_2$  resulted greater than  $Q_1$  (see Table 1), it was deduced that a considerable fraction of P impurities was not electrically active after the predeposition step. The diffused wafers (only

TABLE I Typical values of the junction depth  $X_j$  and of the total amounts  $Q_1$  and  $Q_2$  of electrically active phosphorus (see text), for 25 and 50 min predeposition times.  $X_j$  was measured by the usual angle-lapping and staining technique;  $Q_1$  and  $Q_2$  were obtained by the procedure outlined in [14].

$t$ (min)	$x_j$ ( $\mu\text{m}$ )	$Q_1$ ( $\text{cm}^{-2}$ )	$Q_2$ ( $\text{cm}^{-2}$ )
25	1.1	$1.0 \times 10^{16}$	$2.2 \times 10^{16}$
50	1.8	$1.6 \times 10^{16}$	$3.3 \times 10^{16}$

predeposited) were chemically polished at only one side in order to completely remove the diffused layer and then mounted on the Lang camera with the etched surface directed to the X-ray source.  $\text{CuK}\alpha$  ( $\mu t \sim 4$ ) radiation and in some cases  $\text{MoK}\alpha_1$  ( $\mu t \sim 0.4$ ) radiation were used for recording the topographs on Ilford L4 and G5 nuclear emulsions.

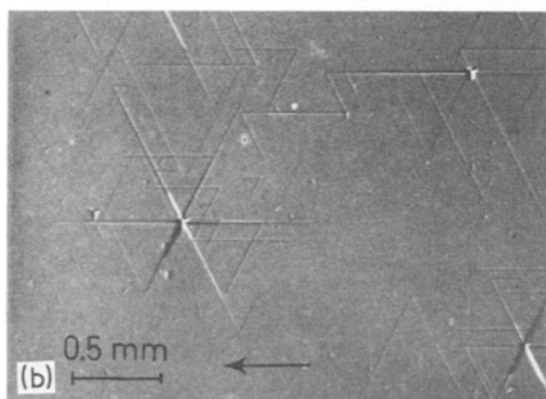
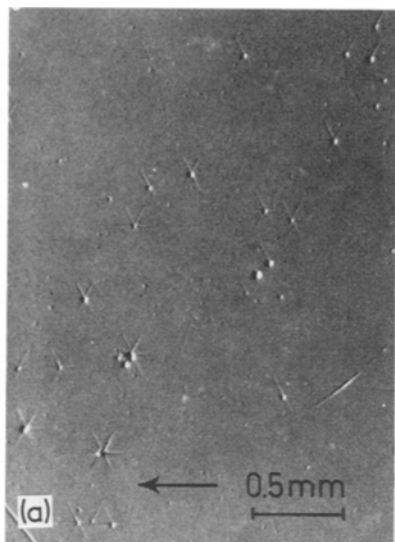


Figure 1 ( $2\bar{2}0$ ) topographs of silicon wafers after (a) 25 min and (b) 50 min phosphorus predeposition.  $\text{CuK}\alpha_1$  radiation.

### 3. Results and discussion

#### 3.1. Contrast of X-ray images

Typical X-ray images of the defects produced during 25 and 50 min predepositions are shown in Fig. 1. The presence of star-like dislocation patterns associated with large precipitates is

clearly displayed. Phosphorus precipitation is not surprising owing to the observed differences between  $Q_2$  and  $Q_1$ . The length of the dislocation lines was observed to increase with increasing diffusion time, therefore the greatest part of the investigations was performed on 50 min samples.

All the dislocation lines were found to lie on the  $\langle 110 \rangle$  directions parallel to the surface of the crystal. Their Burgers vectors were determined by applying the commonly used extinction rules for the contrast to the  $\{220\}$  and  $\{422\}$  symmetrical reflections and to the  $\{111\}$  asymmetrical ones. These dislocations resulted to be of  $60^\circ$  type, with their Burgers vectors parallel to the  $\langle 110 \rangle$  directions lying on the  $(111)$  plane.

The observed X-ray contrast was essentially "Friedel contrast" [7] due to tie-point migration on the dispersion surface [8, 9]. This statement was ascertained by observing inversion of black-white contrast in  $(hkl)$  and  $(\bar{h}\bar{k}\bar{l})$  reflections, as it is shown by comparison between Fig. 1b and Fig. 2. Moreover, "limited projection topographs" obtained with exclusion of the direct component of the image did not show any appreciable difference with those previously reported, and finally  $\text{MoK}\alpha_1$  radiation produced only very feeble contrast. The appearance of "Friedel images" suggested that the observed array of dislocations was close to the exit surface of the crystal [10], as was checked by taking a topograph in a wafer which was locally thinned step-by-step by means of chemical etching. This topograph is given in Fig. 3 which shows that the whole pattern of defects is

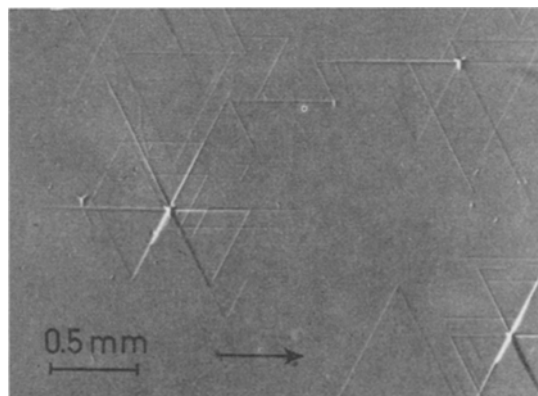


Figure 2 ( $2\bar{2}0$ ) topograph of the same area shown in Fig. 1b. The inversion of the black-white contrast is typical of "Friedel contrast".  $\text{CuK}\alpha_1$  radiation.

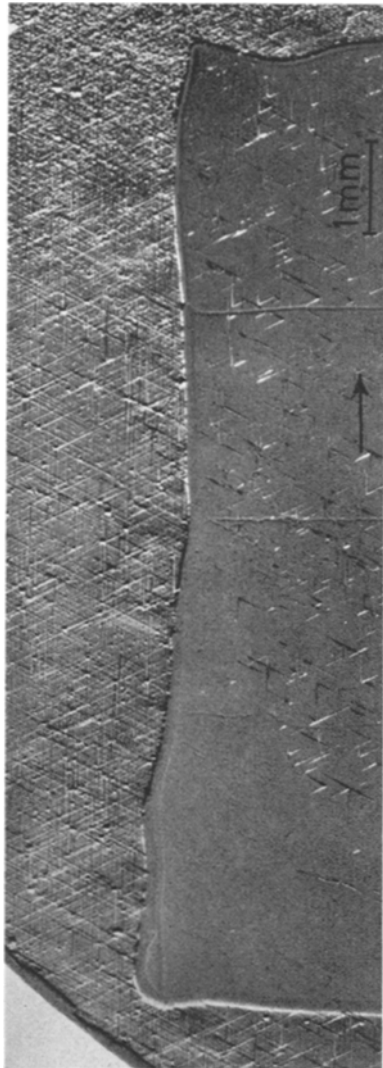


Figure 3 {220} symmetrical L ue topograph of a sample which was chemically thinned step by step. Within the specimen, four steps were obtained of about 0.40, 0.08, 0.05 and 0.02  $\mu\text{m}$  (from the top to the bottom), respectively.  $\text{CuK}\alpha_1$  radiation.

contained within the thickness of the diffused layer. This result, together with the observation that the crystals which were heavily etched before the diffusion treatment did contain a lower density of defects, suggested the hypothesis that phosphorus precipitation took place at sites of surface damage. We believe that the  $60^\circ$  dislocations nucleate at microcracks decorated with phosphorus; in fact, such defects show arms in the  $\langle 112 \rangle$  directions parallel to the traces of

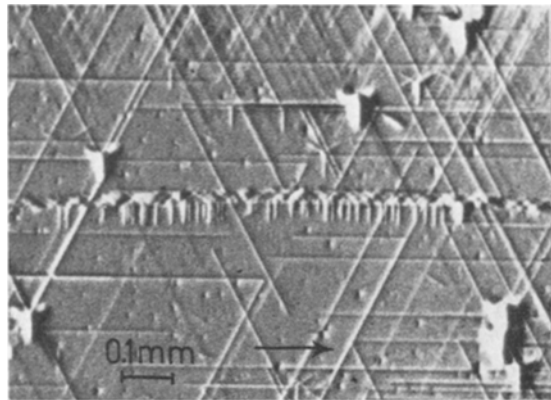


Figure 4 {220} symmetrical L ue topograph showing decorated surface defects which may appear isolated or gathered at accidental scratches.  $\text{CuK}\alpha_1$  radiation.

the  $\{110\}$  cleavage planes and densely populate accidental surface scratches (see Fig. 4).

The analysis of the black and white contrast of the  $60^\circ$  dislocations with respect to the sense of the scattering vector (arrows in the figures) allowed the determination of the sign of a non-compensated curvature of the reflecting planes. The lack of compensation was due to the strong interaction between the dislocations and the crystal surface. The sign of the curvature resulted to be in agreement with the statement that the  $\{111\}$  inclined extra half-plane of each dislocation appeared on the diffused surface of the wafer.

### 3.2. Growth mechanism of dislocations

The hypothesis that the dislocations are generated by plastic relaxation, through glide motion, of the stress concentrated at the nucleating defects is hardly justifiable. In fact, as it is shown in Fig. 1, the length of each dislocation line was observed to increase parallel to the dislocation itself; on the contrary, a glide motion, being parallel to the Burgers vector, would cause a curvature in the ancrated  $60^\circ$  dislocation line. One is then forced to consider climb processes. In order to discuss the generation of dislocation lines by climb one has to consider that an oxide layer about  $10^8 \text{ \AA}$  thick (950  $\text{ \AA}$  and 1400  $\text{ \AA}$  for 25 and 50 min predeposition times, respectively) was formed on the surface of the crystal during the predeposition step. The role of a growing oxide layer on the generation of defects such as stacking-faults and dislocation loops in Si was stressed by Sanders and Dobson [3] and by

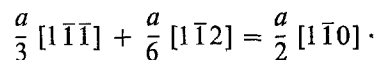
Prussin [5]. Owing to the fact that a vacancy undersaturation is established within the crystal during the oxidation [3, 5], the equilibrium interstitial concentration near the surface will be increased. A vacancy undersaturation is also produced by diffusion of phosphorus impurities which occupy substitutional sites. Vacancy undersaturation causes precipitation of interstitial discs in the  $\{111\}$  planes with subsequent collapse to form extrinsic Frank loops. Prussin [5] has shown that extrinsic Frank loops would preferentially be formed at a number of sites where the tensile stress is greater. According to his treatment the critical vacancy undersaturation to form an extrinsic Frank loop is lowered in the presence of a tensile stress by the amount

$$\exp \left\{ - \frac{P}{K_B T} \frac{\partial V(0)}{\partial n} \right\}$$

where  $P$  is the purely tensile component of the stress state,  $V(0)$  is the volume of vacancy formation at zero pressure and the derivative is taken against the number of vacancies  $n$ . These conditions favour the nucleation of Frank loops at those sites near the surface defects where the tensile stress predominates.

Observations of Frank loops and associated stacking-faults in  $\{111\}$  planes in silicon are commonly performed by means of electron transmission microscopy methods [3, 4, 11]. These defects cannot be observed by X-ray topography owing to the low resolution of this technique ( $\sim 1 \mu\text{m}$ ). In fact a partial Frank loop and its associated stacking fault are more stable than a perfect  $60^\circ$  dislocation only for a sufficiently small loop radius  $r$ . This is due to the fact that the energy of the fault (proportional to  $r^2$ ) grows faster than the energy of dislocation loops (proportional to  $r$ ) so that there is a critical radius for which the energies of the Frank loop and the stacking fault together become larger than that of a perfect dislocation. This critical radius can be estimated to be smaller than the resolution of X-ray techniques [11], so that one can observe the defect only at its final stage, that is a perfect dislocation, as in the present work\*. The process leading to a perfect dislocation is commonly described as a reaction between the Frank sessile dislocation and a Shockley partial dislocation having one of the three  $(a/6) \langle 112 \rangle$  Burgers vectors lying in the fault plane. This

latter is envisaged to be formed inside the loop and then to spread across the loop removing the fault. A typical reaction describing this process is



The final stage is then a star-like pattern of  $60^\circ$  dislocations starting from the nucleating defect and ending at the surface of the crystal, the extra-half plane being a couple of inclined  $\{111\}$  planes, as proposed by Hornstra [12].

In order to clarify the growth mechanism of  $60^\circ$  perfect dislocations, some heating experiments were performed. Owing to the low contribution of the configurational entropy term to its free energy, a dislocation cannot be in thermal equilibrium with the crystal. One then expects that the  $\{111\}$  extra half-planes should dissolve upon heating the sample at a suitable temperature. This process takes place by means of absorption of vacancies at the extra half-plane, that is through a vacancy flux towards the dislocation line causing positive climb. A reduction in the length of the dislocation lines was indeed observed after a 24 h heat-treatment at  $750^\circ\text{C}$  in a pure  $\text{N}_2$  atmosphere of a specimen which was washed in HF in order to strip the oxide layer grown during the phosphorus predeposition, as shown in Fig. 5. The  $\text{N}_2$  atmosphere was used in order not to affect considerably the equilibrium between the crystal and its surface. However, a quite similar result was also obtained after the same heat-treatment was performed in a sample which retained its oxide layer (see Fig. 5). This means that a vacancy flux towards the dislocation line is preserved even when the surface is restricted as a vacancy source. Annealing of dislocation lines was also observed after heating at  $700^\circ\text{C}$  for 80 h and at  $1100^\circ\text{C}$  for 2 h in a 90%  $\text{N}_2$  and 10%  $\text{O}_2$  atmosphere.

A steam oxidation for 20 min at  $920^\circ\text{C}$  was successively performed on the previously mentioned samples in order to grow an oxide layer as nearly thick as the one formed during the P predeposition. Since the dislocation pattern was not appreciably modified (compare Figs. 6 and 5), it was suggested that the vacancy flux towards the surface due to the oxygen diffusion into the lattice during the oxidation is insufficient to reverse climb and to cause a dislocation growth

\*Transmission electron microscopy observations of the same specimens revealed the presence of extrinsic stacking faults associated with precipitates where X-ray topography showed the absence of perfect dislocations. The crystallography of these particles will be the object of future work.

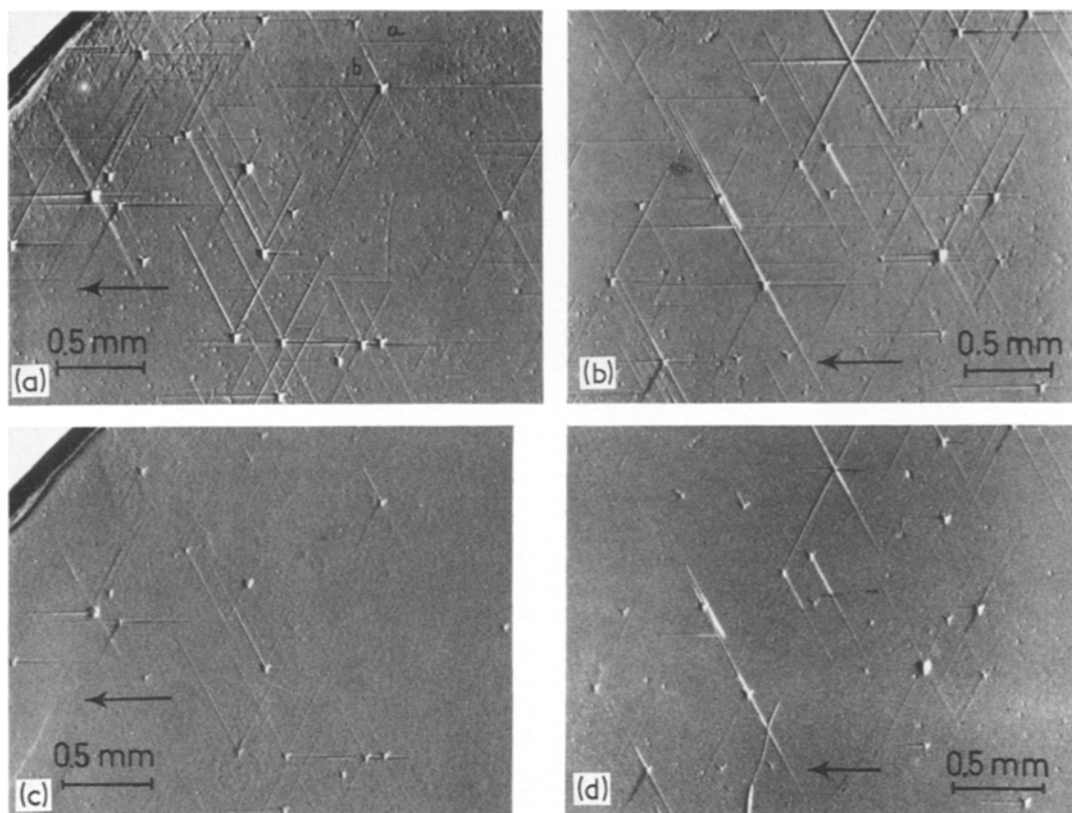


Figure 5 ( $\bar{2}20$ ) topographs.  $\text{CuK}\alpha_1$  radiation. (a) and (b) refer to silicon wafers after a 50 min phosphorus pre-deposition. (c) and (d) refer to the same wafers after a 24 h heating at  $750^\circ\text{C}$  in  $\text{N}_2$  atmosphere. The oxide layer was stripped before heating only in case (c) (see text).

comparable to that produced in the pre-deposition process.

The vacancy flux towards the surface may be considerably enhanced during the pre-deposition step owing to the phosphorus diffusion into the lattice. This process causes a flux which adds to that due to the growing oxide. The whole of the above considerations, as well as the experimental results, indicates that the vacancy flux due to the phosphorus diffusion is mainly responsible for the observed growth of dislocation lines by negative climb during the pre-deposition process.

### 3.3. Dislocation reactions

The  $60^\circ$  dislocations were not always arranged into simple patterns of straight lines. A single line was often observed to have different parts oriented as the different  $\langle 110 \rangle$  directions into the  $(111)$  plane, as shown in Fig. 5a. However, since

the analysis of their X-ray contrast gave different  $\langle 110 \rangle$  Burgers vectors for the different straight portions, these latter were proved to be independent dislocations with Burgers vectors lying in the  $(111)$  plane. Two  $60^\circ$  dislocation lines, such as a and b in Fig. 5a, with Burgers vectors  $(a/2) [\bar{1}01]$  and  $(a/2) [1\bar{1}0]$  respectively, reacted at their common point with a third dislocation with Burgers vectors  $(a/2) [01\bar{1}]$ . Since the extra half-planes belonging to the dislocations a and b are the inclined  $(11\bar{1})$  and  $(\bar{1}11)$  planes, the above reaction may be described as a conversion of the two inclined extra planes one into the other during the growth of the line. This picture requires that the third dislocation line involved in the reaction is parallel to the  $[011]$  inclined direction which is common to the two specified inclined extra planes. This third dislocation whose length is of the order of the thickness of the diffused layer ( $\sim 1 \mu\text{m}$ ) cannot

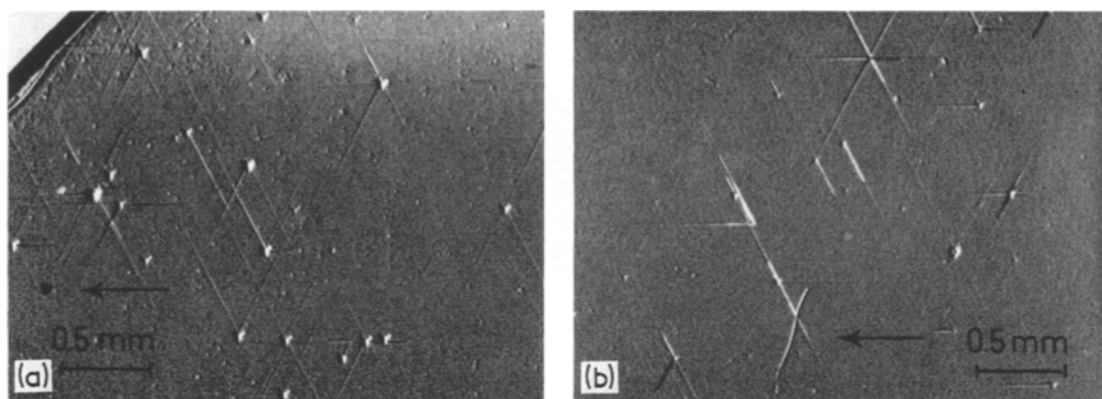


Figure 6 ( $\bar{2}20$ ) topographs of the same Si samples as (c) and (d) in Fig. 5 after a steam oxidation at  $920^{\circ}\text{C}$  for 20 min.  $\text{CuK}\alpha_1$  radiation.

be observed by X-ray techniques, but was indeed evidenced in the same specimens by transmission electron microscopy [13].

#### 4. Conclusion

X-ray topography was employed in order to study the nucleation of dislocation lines at surface heterogeneities in (111) silicon wafers during phosphorus predeposition. Star-like patterns of straight dislocations nucleated at phosphorus decorated surface defects were observed. The dislocation lines and their Burgers vectors resulted to be parallel to the  $\langle 110 \rangle$  directions in the (111) plane, the dislocations being of  $60^{\circ}$  type. The analysis of X-ray contrast, essentially a "Friedel contrast", together with observations after chemical thinning, showed that the inclined  $\{111\}$  extra half-planes appeared on the X-ray exit surface of the crystal and that the whole pattern of defects lied within the diffused layer.

The growth direction of the dislocations suggested the hypothesis of climb processes. It was supposed that vacancy undersaturation due to the predeposition process generated extrinsic Frank loops at sites of greater tensile stress. These loops gave rise to the observed  $60^{\circ}$  dislocations after growing beyond a critical size. Annealing and thermal oxidation experiments suggested that the vacancy flux towards the surface which was due to the P diffusion was mainly responsible for the growth of the  $60^{\circ}$  dislocations by means of negative climb.

#### Acknowledgements

It is a pleasure to thank Dr S. Solmi and Mr P. Negrini of the Laboratorio LAMEL for their kind interest and for the preparation of the silicon wafers. Thanks are also due to Mr A. Zani (lab.LAMEL) for his help in processing the X-ray micrographs.

#### References

1. S. PRUSSIN, *J. Appl. Phys.* **32** (1961) 1876.
2. H. J. QUEISSER, *ibid* **32** (1961) 1776.
3. I. R. SANDERS and P. S. DOBSON, *Phil. Mag.* **20** (1969) 881.
4. K. V. RAVI, *J. Appl. Phys.* **43** (1972) 1785.
5. S. PRUSSIN, *ibid* **43** (1972) 2850.
6. C. M. DRUM and W. VAN GELDER, *ibid* **43** (1972) 4465.
7. G. H. SCHWUTTKE and J. K. HOWARD, *ibid* **39** (1968) 1581.
8. P. PENNING and D. POLDER, *Philips Res. Rep.* **16** (1961) 419.
9. P. PENNING, *ibid (suppl.)* **5** (1966) 1.
10. A. AUTHIER, *Adv. X-ray Anal.* **10** (1967) 9.
11. S. DASH and M. L. JOSHI, *IBM J. Res. Develop.* **14** (1970) 453.
12. J. HORNSTRA, *J. Phys. Chem. Solids* **5** (1958) 129.
13. A. ARMIGLIATO, Lab. LAMEL - CNR, Bologna, Italy, private communication.
14. A. S. GROVE, "Physics and Technology of Semiconductor Devices", Chapter 3 (Wiley and Sons, New York-London-Sydney, 1967).

Received 23 April and accepted 9 May 1974.